

Ethanopharmacological Approach to Control the Replication of 2019-nCov in Host- An Insilico Study

M.Thenmozhi¹, Suma Mohan², M.Sathish Kumar³, S.T.Kumaravel⁴

¹Department of Biotechnology, Selvam College of Technology, Namakkal, India.

²Department of Bioinformatics, SASTRA University, Tanjore.

³Department of Pharmaceutical Technology, Anna University BIT Campus, Tiruchirappalli.

⁴Department of Mechanical Engineering, Paavai Engineering College, Namakkal.

*Correspondence to: Dr.M.Thenmozhi, Department of Biotechnology, Selvam College of Technology, Namakkal, India; Email: thenmozhi.marudhaurai@gmail.com

Received: August 21, 2023; Accepted: October 21, 2023; Published Online: October 25, 2023

How to cite: Thenmozhi M., Mohan S., Kumar M. S., and Kumaravel, S.T. Ethanopharmacological Approach to Control the Replication of 2019-nCov in Host- An Insilico Study. *BME Horizon*, 2023; vol1(2). DOI: [https://doi.org/10.37155/2972-449X-vol1\(2\)-72](https://doi.org/10.37155/2972-449X-vol1(2)-72)

Abstract: 2019- nCoV viral disease threatening every individual throughout the world. It is a highly challenging task to control the spread everywhere. There are certain antiviral drugs, steroids that are currently being prescribed to infected patients for faster recovery. But there is no proper cure today for this pandemic. In this present study, we have focused on controlling the replication and other possibilities of interaction of the 2019-nCoV virus inside the host cells. There are various herbs prescribed to us to improve our immunity and prepare our bodies to fight against this pathogen. In this study, herb compounds that are selected are Andrographolide (AP₁), 14-deoxy-11,12-didehydroandrographolide(AP₃), Ascorbic acid, Cinnamaldehyde, Curcumin, Diallyl sulfide, Eugenol. Gingerol, Kaempferol, Deacetylnimbin, Piperine, Quercetin, thymol, thymoquinone, Vasicine based on the literature survey. Selected ligands are most of them to treat respiratory tract infections and are also related to improving humoral immunity. Selected Ligand was allowed to dock against viral proteins which Crystal Structure of the SARS COV-2 Papain-like protease (Figure 1a) (PDB ID: 6wx4), RNA dependent RNA polymerase (Figure 1b) (PDB ID: 7c2k), Crystal structure of SARS COV-2 ORF7A encoded accessory protein (Figure 1c) (PDB ID: 6w37) Crystal structure of SARS COV-2 ADP-Ribose phosphatase NSP3 Proteins (PDB ID: 6w6y), PDB ID 6zsl Crystal structure of SARS COV-2 helicase NSP13 (PDB ID: 6ZSL), Crystal structure of NSP10-NSP16 Complex (PDB ID: 7bq7), PDB ID 6xdc Crystal structure of SARS COV-2 ORF3a Protein (PDB ID: 6xdc) to study their efficacy to control the replication and possible interactions in the human system using computational docking study. A Protein-Protein interaction study was



© The Author(s) 2023. **Open Access** This article is licensed under a Creative Commons Attribution 4.0 International License (<https://creativecommons.org/licenses/by/4.0/>), which permits unrestricted use, sharing, adaptation, distribution and reproduction in any medium or format, for any purpose, even commercially, as long as you give appropriate credit to the original author(s) and the source, provide a link to the Creative Commons license, and indicate if changes were made.

also performed to study the efficacy of papain enzyme inhibitory efficacy of selected target proteins. Molecular dynamics studies were also performed to ensure the ligand efficacy for the selected target proteins.

Keywords: 2019-nCoV; Target proteins; Docking; Dynamics; Ligand efficacy

1. Introduction

2019-nCoV viral strain is a new edition of the coronavirus family. *Coronaviridae* is a family of novel corona viral strains. It belongs to RNA viruses. Nowadays many anti-viral drugs, steroids are practicing to treat them to control the disease but it works differently with patients some may get cured others may continue to suffer^[1]. This viral genome expresses many proteins and it happens to interact with human host cells. There are various docking studies to carried out on envelop proteins. This present study focuses on three target proteins which are as follows Crystal Structure of the SARS COV-2 Papain-like protease (**Figure 1a**) (PDB ID: 6wx4), RNA dependent RNA polymerase (**Figure 1b**) (PDB ID: 7c2k), Crystal structure of SARS COV-2 ORF7A encoded accessory protein (**Figure 1c**) (PDB ID: 6w37) Crystal structure of SARS COV-2 ADP-Ribose phosphatase NSP3 Proteins (PDB ID: 6w6y), PDB ID 6zsl Crystal structure of SARS COV-2 helicase NSP13 (PDB ID: 6ZSL), Crystal structure of NSP10-NSP16 Complex (PDB ID: 7bq7), PDB ID 6xdc Crystal structure of SARS COV-2 ORF3a Protein (PDB ID: 6xdc) helped the virus to replicate in the host system^[2]. papain-like protease is one of the two important proteases in the viral genome. papain-like protease helps in the virus replication process and helps to destroy the viral response in the deubiquitination of host cell factors. The papain-like protease one of the targets for antiviral development processes^[3].

RNA-dependent RNA polymerase is one of the important proteins in viral replication. It is a central compartment of viral replication and transcription machinery. It is one of the targets for antiviral drugs^[4,5].

Orf7A is one of the open reading frame proteins in nCov19. ORF7A inhibits the activity of Bone Marrow Stromal Protein-2 (BST-2) which plays an important role in viral infections. It controls the release of virions into the system. Inactivation of BST-2 leads to the down-regulation in the inflammatory response. Inhibiting ORF7A helps to retain the BST-2 activity^[6]. NSP3 is one of the important Non-structural proteins

it plays a major role in host immune response. By inhibiting this NSP3 protein helps to preserve humoral immune response. ORF3a is one of the potential targets in treating nCov19 infection. ORF3a plays important role in viral pathogenicity^[7].

NSP13 is one of the important targets in controlling nCov19 infection. Studies showed that this hydrolase protein NSP13 plays a major role in this viral replication in the host cell^[8]. NSP10-NSP16 Protein complex possesses 2' – O-MTase activity which helps in host viral replication. So it may be one of the potential targets in nCov19 infection. Papain enzyme known for its medicinal value in this study papain enzyme docked against selected target proteins and study the efficacy of papain enzyme selected target proteins^[9].

This present study investigates the selected target proteins that will be docked against selected ligand molecules that are using traditionally to boost the immune system and also to treat the common cold and mild infections.

Selected ligands must be tested for their drug-likeness property. It is important to analyze the selected ligands should obey Lipinski's rule of five. It helps to analyze the stability of the compound and ensures the ability to exhibit the proposed biological activity in our system. Based on Lipinski's rule the selected compounds ensure whether the selected ligand molecules will be orally active or not^[10,11,12].

So far various computational studies carried out on main protease protein, Angiotensin converter proteins, nucleocapsid proteins, based on these studies in this study differ from other studies because the viral entry into our body is inevitable^[13, 14, 15, 16, 17, 18, 19].

This present study deals with the viral protein interactions inside the host. Viral-host interaction mediates viral replication and other processes. Blocking viral–host interacting proteins helps to control the viral infection is the strategy of this present study. Other host-viral interacting proteins are like other open reading frame proteins and other non-structural proteins with screened ligands studies were also performed^[20,21,22].

2. Materials and Methods

2.1 ADME/T Property Analysis

The drug-likeness property of selected ligand molecules was assessed using the webserver <http://www.scfbio-iitd.res.in/software/drugdesign/lipinski.jsp>^[23].

2.2 Protein preparation

The 3D structure of target proteins was Crystal Structure of the SARS COV-2 Papain-like protease (**Figure 1a**) (PDB ID: 6wx4), RNA dependent RNA polymerase (**Figure 1b**) (PDB ID: 7c2k), Crystal

structure of SARS COV-2 ORF7A encoded accessory protein (**Figure 1c**) (PDB ID: 6w37) Crystal structure of SARS COV-2 ADP-Ribose phosphatase NSP3 Proteins (PDB ID: 6w6y), PDB ID 6zsl Crystal structure of SARS COV-2 helicase NSP13 (PDB ID: 6ZSL), Crystal structure of NSP10-NSP16 Complex (PDB ID: 7bq7), PDB ID 6xdc Crystal structure of SARS COV-2 ORF3a Protein (PDB ID: 6xdc) were downloaded from Protein Data Bank (www.rcsb.org/pdb)^[24,25,26,27].

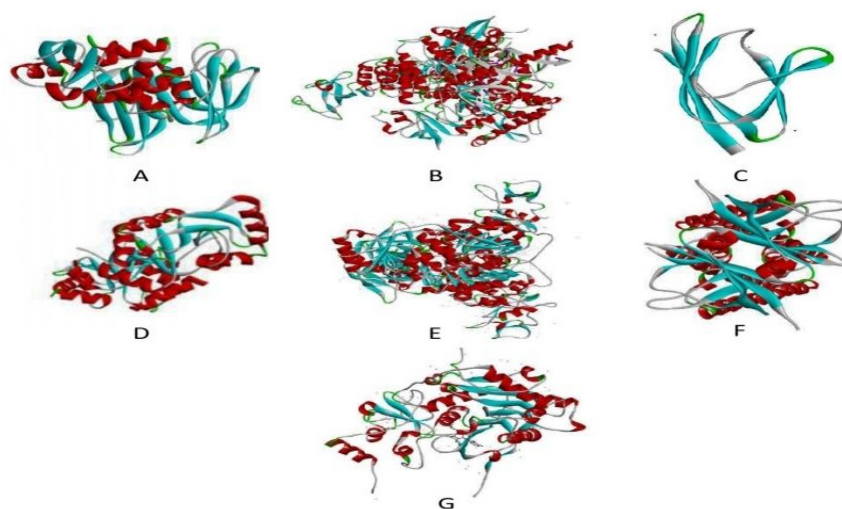


Figure 1: (a) PDB ID 6wx4 Crystal Structure of the SARS COV-2 Papain-like protease; (b) PDB ID 7c2k RNA Dependent RNA Polymerase; (c) PDB ID 6w37 Crystal structure of SARS COV-2 ORF7A encoded accessory protein; (d) PDB ID 6w6y Crystal structure of SARS COV-2 ADP-Ribose phosphatase NSP3 Proteins; (e) PDB ID 6xdc Crystal structure of SARS COV-2 ORF3a Protein; (f) PDB ID 6zsl Crystal structure of SARS COV-2 helicase NSP13; (g) PDB ID 7bq7 Crystal structure of NSP10-NSP16 Complex.

2.3 Ligand Structures

The ligand selection is based on herbs that are used to treat the common cold. In this present study, these ligands were selected to study the efficiency of selected target proteins. There were no studies performed

before with these target proteins against selected target proteins. Ligand structures were downloaded from the PubChem database. (**Table 1**) (<https://www.pubchem.ncbi.nlm.nih.gov>)^[28,29,30,31,32,33,34,35,36,37,38,39,40,41].

Table 1. Chemical Compound and their PUBCHEMID

S.No	Source	Chemical Compound	PUBCHEMID
1	Nilavembu	Andrographolide (AP ₁),	5318517
2	Nilavembu	14-deoxy-11,12-didehydroandrographolide(AP ₃)	17650544
3	Citrus Fruits	Ascorbic acid	54670067
4	Cinnamon	Cinnamaldehyde	637511
5	Turmeric	Curcumin	969516
6	Garlic	Diallyl sulfide	11617
7	Cloves	Eugenol	3314
8	Ginger	Gingerol	442793

Continuation Table:

S.No	Source	Chemical Compound	PUBCHEMID
9	Green leafy Vegetables	Kaempferol	5280863
10	Neem leaves	Nimbin	108058
11	Black Pepper	Piperine	638024
12	Onions	Quercetin	5280343
13	Tulsi leaves	Thymol	6989
14	Black cumin Seeds	Thymoquinone	10281
15	Adathoda Leaves	Vasicine	72610

2.4 Molecular Docking

The protein structure was downloaded and prepared using autodock software, where Kollman charges and polar hydrogen were added and converted the structure format to “.pdbqt” file format. The ligand was prepared by detecting the rotatable bonds and set the aromatic criterion, and the ligand structure format converted to “.pdbqt” format. The Grid parameter file should get prepared for further docking study. Grid generated by selecting grid size, Crystal structure of SARS COV-2 helicase NSP13 (PDB ID: 6ZSL)-90x90x90, Crystal structure of SARS COV-2 ADP-Ribose phosphatase NSP3 Proteins (PDB ID: 6w6y)-80x80x80, Crystal structure of SARS COV-2 ORF3a Protein (PDB ID: 6xdc) - 90x90x90, RNA dependent RNA Polymerase-70x70x70, Crystal structure of SARS COV-2 ORF7A encoded accessory protein (PDB ID: 6w37)-60x70x60, Crystal structure of NSP10-NSP16 Complex-80x80x80, Crystal Structure of the SARS COV-2 Papain-like protease (PDB ID: 6wx4)80x70x80 before performing docking study. Grid size helps the ligand to identify its binding pocket. Docking parameter file should get prepared for docking calculations by choosing macromolecule, as well as ligand file and finally docking parameter file written using the Lamrickan algorithm.

2.5 Protein-Protein Interaction Studies

Target proteins which are as follow Crystal Structure of the SARS COV-2 Papain-like protease (PDB ID: 6wx4), RNA dependent RNA polymerase (PDB ID:

7c2k), Crystal structure of SARS COV-2 ORF7A encoded accessory protein (PDB ID: 6w37) Crystal structure of SARS COV-2 ADP-Ribose phosphatase NSP3 Proteins (PDB ID: 6w6y), Crystal structure of SARS COV-2 helicase NSP13 (PDB ID: 6ZSL), Crystal structure of NSP10-NSP16 Complex (PDB ID: 7bq7), Crystal structure of SARS COV-2 ORF3a Protein (PDB ID: 6xdc) were docked against Papain enzyme which is known for its therapeutic activity using protein-protein docking server PyDock.

2.6 Molecular Dynamics Simulations

In our study, we performed molecular dynamics simulations of protein-ligand, protein-protein complexes using DESMOND and GROMACS 4.0.6 software package. OPLSAA and charmm forcefields were used for preparing the complexes and a 300 K constant temperature was maintained for the simulations. The molecular simulation time of protein-ligand, protein-protein complexes was set at 50ns and 30ns. xmgrace software was used to plot the RMSD graphs.

3. Results and Discussion

3.1 ADME/T Prediction

The drug-likeness property of selected ligands was analyzed so that it ensures oral bioavailability in the human system. Based on the results all the ligands were obeying the rule of five. Results ensured that the selected ligands are exhibits the intended property in the human system (**Table2**).

Table 2. ADME/T analysis results

S, No	Chemical Compound	Mass < 500	Hydrogen bond donor < 5	Hydrogen bond acceptor < 10	Logp < 5	Molar refractivity 40-130
1	Andrographolide (AP ₁),	350	3	5	1.962	93.560
2	14-deoxy-11,12-didehydroandrographolide(AP ₃)	332.0	2	4	2.767	92.076

Continuation Table:

S, No	Chemical Compound	Mass < 500	Hydrogen bond donor < 5	Hydrogen bond acceptor < 10	Logp < 5	Molar refractivity 40-130
3	Ascorbic acid	176.00	4	6	-1.40	35.25
4	Cinnamaldehyde	132	0	1	1.898	41.539
5	Curcumin	368	2	6	3.369	102.01
6	Diallyl sulphide	114.0	0	0	2.09	37.71
7	Eugenol	164.0	1	2	2.12	48.55
8	Gingerol	294.0	2	4	3.23	82.75
9	Kaempferol	286.0	4	6	2.30	72.38
10	Nimbin	498	1	8	3.35	127.53
11	Piperine	285	0	4	2.99	81.16
12	Quercetin	302.0	5	7	2.01	74.05
13	Thymol	150.0	1	1	2.82	46.93
14	Thymoquinone	164.0	0	2	1.66	46.69
15	Vasicine	188	1	3	1.29	54.57

3.2 Protein-ligand Interactions

3.2.1 Crystal structure of the SARS COV-2 papain-like protease

Papain-like protease protein is one of the target proteins in this docking study. Ligands were selected based rationale based on their previous experimental studies for different diseases. Inhibitor efficiency of the selected ligands based on the binding affinity and hydrogen bonds formed in the active site pocket. Based on the Score Nimbin > Piperine > 14-deoxy-11,12-didehydroandrographolide (AP₃) > andrographolide (AP₁) > Quercetin > Kaempferol > Curcumin > Vasicine > Thymoquinone > Cinnamaldehyde > Ascorbic acid > thymol > Eugenol > Gingerol > Diallylsulfide. Based on the hydrogen bond interactions we found that selected ligands were docked in the S1/S2 binding pockets which are said to be the active site pocket of papain-like protease (Rut *et al.*, 2020). HIS73, ARG 82, ILE123, GLU124, LEU125, PHE127, ASP156, ASP164, ARG166, GLN174, HIS175, LEU178, LYS200, VAL202, GLU203, TYR273, THR301 (**Table 3**). Piperine is a potential ligand structure base on its clinically proven therapeutic activity. It showed better binding affinity but it made no hydrogen bond with active site residues (**Figure 2a**).

3.2.2 RNA dependent RNA polymerase

RNA-dependent RNA polymerase was docked against a set of ligands and the results were analyses based on the binding affinity. Nimbin > andrographolide (AP₁) >

curcumin > 14-deoxy-11,12-didehydroandrographolide (AP₃) > Kaempferol > Piperine > Quercetin > Gingerol > Vasicine > Thymol > Thymoquinone > Cinnamaldehyde > Eugenol > Ascorbic acid > diallylsulfide. All the ligands were bound well in the binding pocket of RNA-dependent RNA polymerase (**Figure 2b**). PHE165, TYR169, LYS545, ARG553, ARG555, THR556, TYR619, SER681, THR680, CYS622, ARG624, ASP542, ASP618, ASP760, LYS621, ASP 452, LYS200, GLU203, VAL202. Based on the scores and interactions of Nimbin (**Figure 3b**), the lead molecules for the inhibition of RNA dependent RNA Polymerase (**Table 3**).

3.2.3 Crystal structure of SARS COV-2 ORF7A encoded accessory protein

ORF7A protein results are Piperine > ANDROGRAPHOLIDE (AP₁) > Nimbin > 14-DEOXY-11,12-DIDEHYDROANDROGRAPHOLIDE (AP₃) > Cinnamaldehyde > Kaempferol > Vasicine > Curcumin > Gingerol > thymoquinone > eugenol > Quercetin > thymol > Ascorbic acid > diallylsulfide ranked according to their binding affinity. Based on the score Piperine (**Figure 2c**) exhibits better binding affinity and based on the interactions it bound well in the active site pocket. HIS4, TYR5, GLN 6, LYS17, GLU 18, ASN 28, TYR 60, GLN 61. These amino acid residues are interacting residues found in top-scoring docked poses [**Table 3**].

3.2.4 Crystal structure of SARS COV-2 ADP-Ribose phosphatase NSP3 proteins

NSP3 Protein was docked against selected ligands

and it was docked well in the active site of the NSP3 protein. PHE6, GLY8, TYR9, LYS11, LYS19, GLU120, TYR152, TYR161(**Figure 2d**) are the interacting residues found in top-ranked docking poses. Nimbin was the top-ranked docking pose with greater binding affinity compared with other ligand structures (**Table 3**).

3.2.5 Crystal structure of SARS COV-2 helicase NSP13

NSP13 protein was docked against selected ligand structures. Based on the docking score and interacting amino acids confirmed that the ligands are bound well in the active site of the proteins. From all the results Nimbin structure binding affinity better than other ligand structures (**Table 3**). It may have the inhibitory effect of the NSP13 protein thereby controlling the nCoV19 infection. LYS146, VAL181, LYS192, GLN194, THR214, SER229, MET 233, SER236, ALA237, VAL340, CYS342, ASP344, THR351, LEU363, ARG390(**Figure 3e**).

3.2.6 Crystal structure of NSP10-NSP16 complex

NSP10-NSP16 complex was docked against the

selected ligand structures and top-ranked docking poses have interacted with the following amino acid residues MET42, ASN43, THR47, HIS48, THR58, PRO59, ASP75, LYS76, ARG86, GLN87, ASN101, TYR132, LYS170, ASN198, SER201, ASN198(**Figure 3f**). Based on the docking score piperine was found to be a higher score than other ligand structures (**Table 3**). It may exhibit inhibitory efficacy against the NSP10-NSP16 complex.

3.2.7 Crystal structure of SARS COV-2 ORF3a protein

ORF3a protein was docked against the selected ligand structures and it bound well in the active site of the protein (ORF3a). Top-ranked docked poses have interacted with the following amino acid residues SER60, ILE63, THR64, LYS66, LYS75, HIS78, ARG122, ASP142, ARG126, ARG122, ASP142, ASN144, TYR189, SER205, TYR206 (**Figure 2g**). Based on the binding affinity quercetin exhibits better binding affinity towards ORF3a protein compared with other ligand structures (**Table 3**).

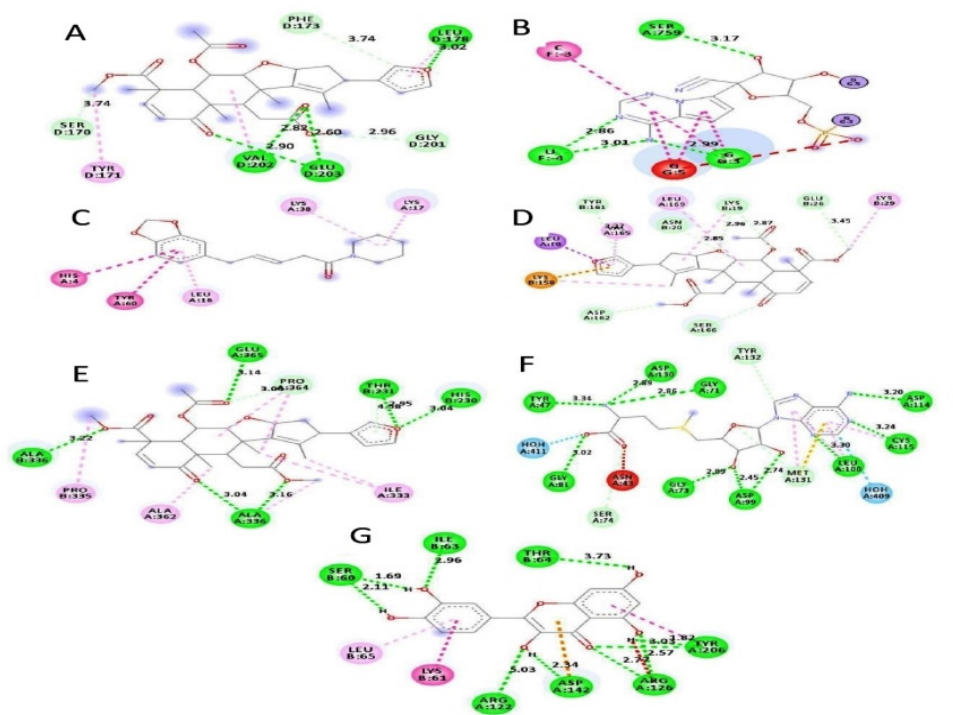


Figure 2: (a) Papain like Protease protein docked with Nimbin interacting residues; (b) RNA Dependent RNA polymerase interacting residues with Deacetylnimbin; (c) ORF7A accessory protein-interacting residues with piperine; (d) NSP3 protein-interacting residues with Nimbin; (e) NSP13 protein-interacting residues with Nimbin; (f) NSP10-NSP16 protein-interacting residues with Piperine; (g) ORF3A accessory protein-interacting residues with Quercetin

Table 3. Molecular docking score and interacting residues for selected target proteins

S.No	Ligand Name	Binding Affinity KJ/mol						
		PDBID 6wx4	PDBID 7C2K	PDBID 6w37	PDBID 6w6y	PDBID 6zsl	PDBID 7bq7	PDBID 6xdc
1	Andrographolide (AP ₁),	-6.24	-8.17	-6.46	-6.99	-6.83	-5.34	-6.82
2	14-deoxy-11,12-didehydroandrographolide(AP ₃)	-6.53	-7.69	-6.26	-7.02	-6.39	-6.4	-7.05
3	Ascorbic acid	-4.64	-4.27	-3.54	-5.57	-4.24	-4.82	-4.02
4	Cinnamaldehyde	-4.75	-4.73	-5.85	-4.82	-5.05	-5.19	-4.12
5	Curcumin	-5.4	-7.84	-5.17	-6.7	-7.02	-5.66	-7.09
6	Diallylsulfide	-3.5	-3.36	-3.42	-3.36	-2.8	-3.75	-3.87
7	Eugenol	-4.54	-4.57	-4.83	-5.46	-3.3	-4.71	-4.39
8	Gingerol	-3.93	-5.42	-5.05	-6.54	-4.38	-3.58	-4.74
9	Kaempferol	-5.76	-7.33	-5.74	-7.35	-7.06	-5.13	-6.75
10	Nimbin	-6.89	-8.55	-6.03	-7.95	-8.16	-5.65	-7.08
11	Piperine	-6.77	-7.26	-6.6	-7.34	-6.92	-7.1	-7.22
12	Quercetin	-5.82	-7.16	-4.49	-7.23	-6.95	-6.14	-7.36
13	Thymol	-4.62	-5.12	-4.26	-6.64	-5.28	-5.42	-5.09
14	Thymoquinone	-4.93	-4.84	-4.91	-6.5	-5.03	-5.45	-4.97
15	Vasicine	-5.25	-5.25	-5.44	-6.17	-6.22	-5.61	-5.25

3.3 Protein-Protein Interaction Study

Papain Enzyme has interacted with target proteins. Papain enzyme ASN64, TYR61, ARG59, TYR67, GLN112, SER205 interacted with amino acid residues of nCov19papain like protease enzyme TYR137, ARG138, TYR71, LEU16, ASN15. Interacting residues were found in the active site of papain-like protease protein (**Figure 3a**). In Papain enzyme and RNA dependent, RNA polymerase docking following papain enzyme amino acid residues which are as follows GLN112 and TYR116 have interacted with GLN444 and ALA 443 of RNA dependent RNA polymerase enzyme (**Figure 3b**).

Papain enzyme ASN117, ARG191, ILE1 made hydrogen bonds with the following amino acid residues from the nCov19 ORF7A which are as follows TYR5, GLU1, PRO9, and HIS58. Interacting residues were in the active sites of the ORF7A protein (**Figure 3c**).

Papain enzyme SER216, THR223, SER58, GLN116 made hydrogen bonds with the following amino acid

residues from the nCoV ORF3A which are as follows THR223, SER216, GLN116, SER58. Interacting residues were in the active sites of ORF3A protein (**Figure 3d**).

Papain enzyme TYR116, ASN155, TYR59 made hydrogen bonds with the following amino acid residues from the nCoV NSP3 protein which are as follows PHE475, TYR476, GLU591 were in the active sites of NSP3 protein (**Figure 3e**).

Papain enzyme GLY94, ALA71, TYR96, LEU45, LYS93 made hydrogen bonds with the following amino acid residues from the nCoV NSP10-NSP16 protein which are as follows ASP106, ARG86, ALA83, GLN87, ALA107, LYS38 were in the active sites of NSP10-NSP16 protein. (**Figure 3f**).

Papain enzyme TYR61, ARG59 made hydrogen bonds with amino acid residues from the nCoV NSP3 protein which are as follows VAL49, GLY 48. Interacting residues were found in the active site of the target protein (**Figure 3g**).

Table 4. Protein-Protein interactions scores

S.No	Protein-Protein Name	Electrostatics	Desolvation	VdW
1	Papain Enzyme with Papain like protease	-19.817	-16.732	41.674
2	Papain enzyme-RNA polymerase	-4.021	-33.997	25.399
3	Papain enzyme-ORF7A	-7.718	-8.886	51.944
4	Papain enzyme-NSP3	-19.996	-5.998	6.178

S.No	Protein-Protein Name	Electrostatics	Desolvation	VdW
5	Papain enzyme-NSP13	-4.811	-33.826	81.689
6	Papain enzyme- NSP10-NSP16 complex	-5.852	-32.194	23.797
7	Papain enzyme – ORF3a	-2.594	-58.224	20.159

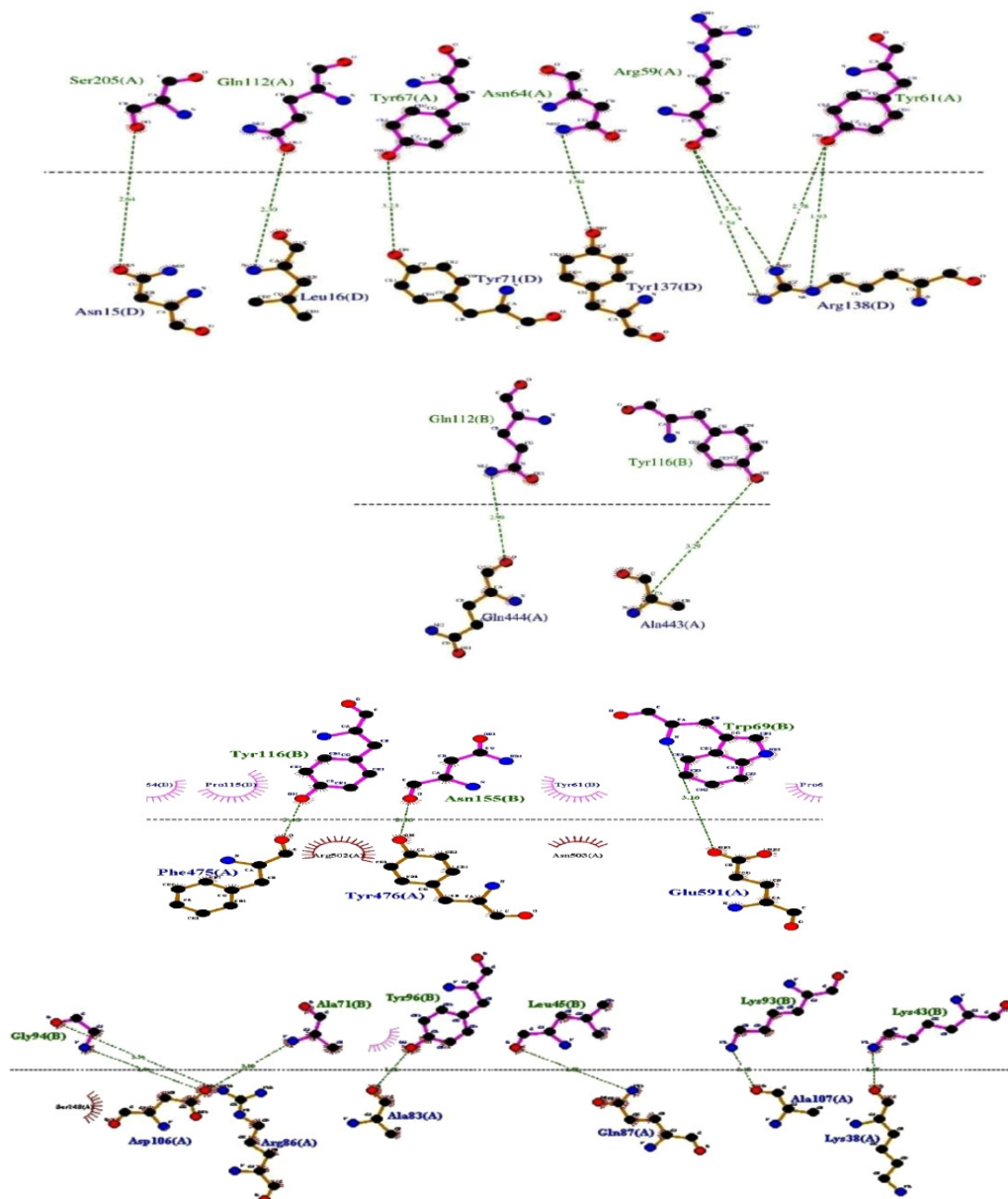


Figure 3. Protein-Protein interactions of (a) Papain enzyme with Papain like Protease, (b) Papain enzyme with RNA dependent RNA polymerase, (c) Papain enzyme with ORF7A protein, (d) Papain enzyme with ORF3A, (e) Papain enzyme with NSP13, (f) Papain enzyme with NSP10-NSP16, (g) Papain enzyme with NSP3

3.4 Molecular dynamics simulations interpretation of docked complexes

In the molecular dynamics simulations, we used the RMSD of the backbone to examine whether the system

reaches its stability and equilibrium. The prepared complexes were immersed in a periodic water box, ions added to the box and the equilibration was performed at 200k constantly. The final molecular dynamics was

performed for 30ns for all the protein-protein and 50ns for protein-ligand complexes. **Figure 4** shows that the RMSD plot for 6w37-9pap complexes (red- protein,

black –protein with ligand), its shows the stability of the protein-protein complex.

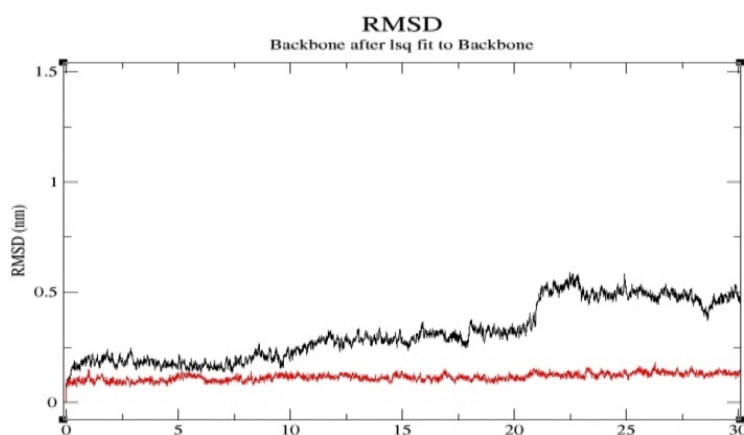


Figure 4. RMSD plot for 6w37-9pap complexes (red- protein, black –protein with ligand)

The RMSD of the 6w37-piperine complex shows the stable conformation after 25ns from starting point of the stimulation and it represents the steady-state up to 50ns (**Figure 5 (a)**). The RMSF of the protein and ligand plot shows the local characteristic changes and positions (**Figure 5(b),(c)**). Protein secondary structures like alpha-helix and beta-strands were interpreting throughout the simulations, alpha helices highlighted with red color and blue color indicates the beta-strands, and SSE plots show the residue index

throughout the simulation (**Figure 5 (d)**). From the SSE plots, the residue index shows beta-strands completely. The protein-ligand contacts (**Figure 5 (e)**) show the bond interaction with the residues, hydrophobic interactions found with HIS4, VAL14, LEU15, LEU16, PHE48, TYR60, LEU62 residues. The hydrogen bond interactions were found with GLN6, LYS17, GLN61 residues, and only one water bridge was found with LYS17 and no ionic interactions were found between the protein-ligand.

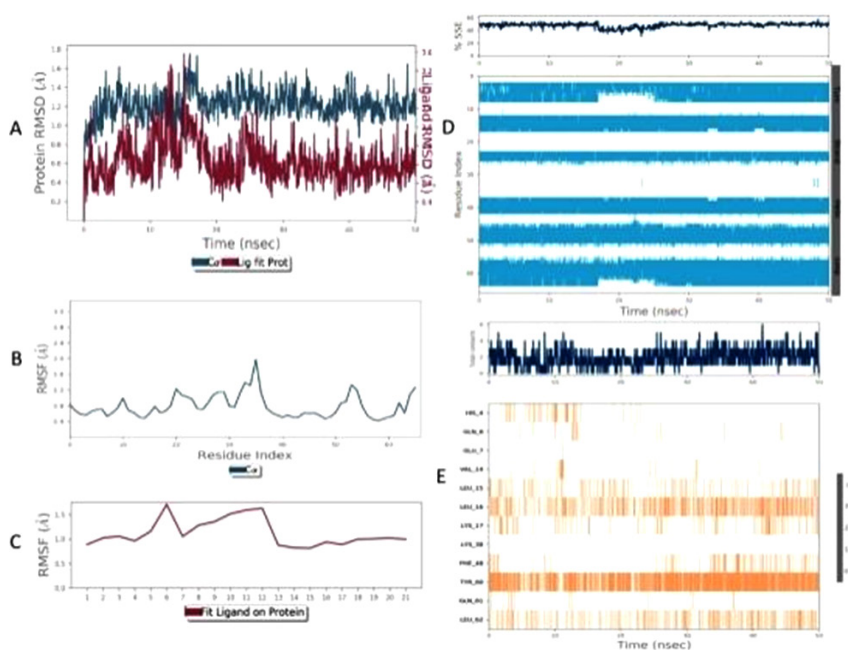


Figure 5: (a) RMSD plot for 6w37-piperine complex (red- protein, black –protein with ligand); (b) protein RMSF; (c) Ligand on protein RMSF; (d) Structure stability of the protein-ligand complex; (e) Protein residue contacts with ligand.

The RMSD of the nsp16-piperine complex shows the stable conformation after 30ns from starting point of the stimulation and it represents the steady-state up to 50ns (**Figure 6 (a)**). The RMSF of the protein and ligand plot shows characteristic changes and positions (**Figure 6(b),(c)**). Protein secondary structures like alpha-helix and beta-strands were interpreting throughout the simulations, alpha helices highlighted with red color and blue color indicates the beta-strands, and SSE plots show the residue index throughout the simulation (**Figure 6(d)**). From the SSE plots, the residue index shows beta-strands and alpha helices equally found.

The protein-ligand contacts (**Figure 6(e)**) show the bond interaction with the residues, hydrophobic interactions found with PRO80, LEU100, MET131, PHE149 residues. The hydrogen bond interactions found with ASN43, GLY71, ALA72, GLY73, GY81, ASP99, LEU100, ASN101, ASP114, CYS115, ASP30, TYR132 residues, water bridges found with ASN43, LYS46, HIS69, PHE70, ALA72, GLY73, SER74, ASP75, LYS76, THR82, ASP98, ASN101, ASP114, ASP115, ASP130, MET131, ASP133, LYS135, LYS170, ASN297, and ionic interactions found with LYS46, ASP130, ASP133 residues.

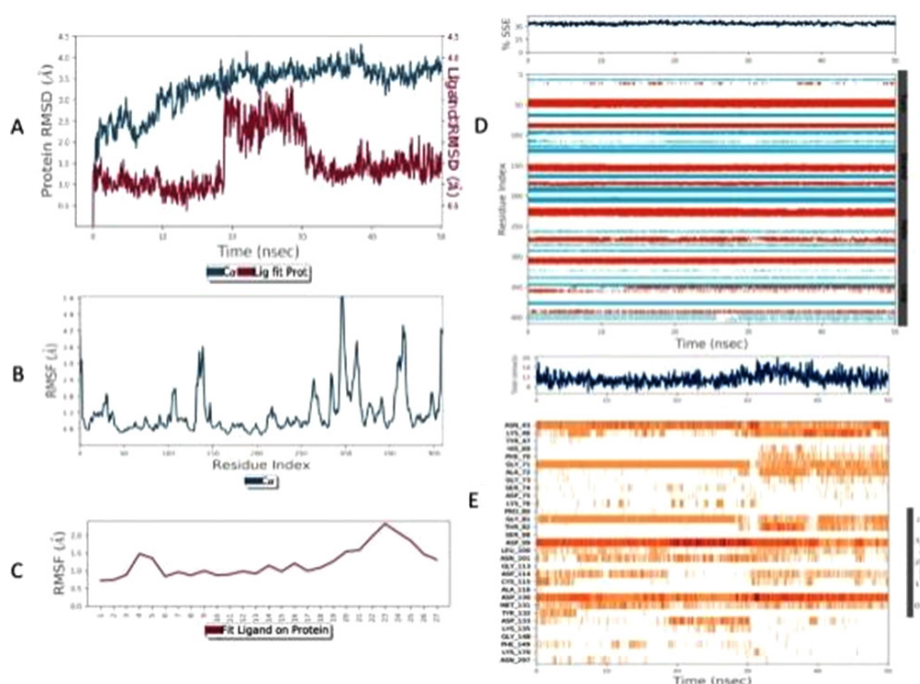


Figure6: (a) RMSD plot for nsp16-piperine complex (red- protein, black –protein with ligand); (b) protein RMSF; (c) Ligand on protein RMSF; (d) Structure stability of the protein-ligand complex; (e) Protein residue contacts with ligand.

4. Conclusion

This present study deals with the computational docking study using small molecules and an enzyme to control the replication of the virus in the host cell. Selected small molecules were studied for their drug-likeness property because they are herbal-based compounds. Based on this study Nimbin, Piperine and Quercetin are the lead molecules that were bound well in the active site of target proteins (Papain-like protease, RNA dependent RNA Polymerase, ORF7A protein, NSP3, NSP13, NSP10-NSP16, ORF3A). Based on the Scores and interactions ensure the binding

affinity and protein-ligand stability. It ensures that the lead molecules were strong enough to inhibit the target proteins. Papain enzyme was also docked against the selected target proteins using the Protein-Protein interaction server. Molecular dynamics studies were performed for the proteins NSP13, 6w37 with piperine ligand results were ensured that the ligand can inhibit the target proteins. In the same way, protein-protein dynamics studies were also performed and ensured that the papain enzyme structure also can control the target protein ORF7A. This present study was performed to choose multiple targets to control the infection with studied ligand structures.

Acknowledgement

I express sincere gratitude to SASTRA Deemed to be University for Schrodinger software (<https://www.schrodinger.com/>) support Maestro and desmond versions used maestrov12.3, desmond-v5.6.

Authors' Contributions

Work Planned, Docking, Material collection were performed by M.Thenmozhi, Protein-Protein dynamics & Image editing were performed by M.Sathishkumar, Protein- ligand dynamics was performed by Suma mohan, Proof reading and literature support were performed by S.T.Kumaravel. All the authors contributed to the study conception and design and approved the final manuscript.

Conflicts of Interest

Not applicable

Declarations

Funding: Not Applicable

Availability of data and material: Not Applicable

Code availability: Not Applicable

References

- [1] Yu R., Chen L. and Lan R. Computational screening of antagonists against the SARS-CoV-2 (COVID19) coronavirus by molecular docking. *International journal of antimicrobial agents*, 2020; <https://doi.org/10.1016/j.ijantimicag.2020.106012>.
- [2] Barik A., Raj G. and Modi G. Molecular docking and binding mode analysis of selected FDA approved drugs against COVID-19 selected key protein targets: An effort towards drug repurposing to identify the combination therapy to combat COVID-19. preprint, 2020; arXiv;2004.06447
- [3] Rut W., Zmudzinski M., Lv Z, *et al.* Activity profiling of SARS-Cov-2-PLpro protease provides a structural framework for anti-COVID-19 drug design. *Science advances*, 2020; 6(42): 1-12.
- [4] Ishihama A. and Barbier A. Molecular anatomy of viral RNA-directed RNA polymerases. *Archives of virology*, 1994;134 : 235-258.
- [5] Wang Q., Wu J., Wang H., *et al.* Structural basis for RNA replication by the SARS-CoV-2 Polymerase. *Cell*, 2020; <https://doi.org/10.1016/j.cell.2020.05.034>.
- [6] Taylor JK., Coleman CM., Postel S., *et al.* Severe acute respiratory syndrome coronavirus ORF7a inhibits bone marrow stromal antigen 2 virion tethering through a novel mechanism of glycosylation interference. *Journal of virology*, 2015; 89: 11820-11833.
- [7] Gordon D.E., Jang G.M., Bouhaddou M., *et al.* A SARS-CoV-2 protein interaction map reveals targets for drug repurposing. *Nature*, 2020; 583:459–468. <https://doi.org/10.1038/s41586-020-2286-9>
- [8] Mirza MU. and Froeyen M. Structural elucidation of SARS-CoV-2 vital proteins: Computational methods reveal potential drug candidates against main protease, NSP12 polymerase, and NSP13 helicase. *Journal of pharmaceutical analytics*, <https://doi.org/10.1016/j.jpha.2020.04.008>.
- [9] LaLonde JM., Zhao B., Smith WW., *et al.* Use of papain as a model for the structure-based design of cathepsin K inhibitors: crystal structures of two papain-inhibitor complexes demonstrate binding to S'-Subsites. *Journal of Medicinal Chemistry*, 1998; 41:4567-4576.
- [10] Lipinski CA., Lombard F., Dominy BW., *et al.* Experimental and computational approaches to estimate solubility and permeability in drug discovery. *Advanced drug delivery reviews*, 2001; 46:3-26.
- [11] Ghose AK., Viswanadhan VN. and Wendoloski JJ. A knowledge-based approach in designing combinatorial or medicinal chemistry libraries for drug discovery. *Journal of combinatorial chemistry*, 1999; 1(1):55-68. <https://doi.org/10.1021/cc9800071>.
- [12] Smith G F. Designing drugs to avoid toxicity. *Progress in medicinal chemistry*, 2011; 50(1): 1-47. <https://doi.org/10.1016/B978-0-12-381290-2.00001-X>.
- [13] Arya R., Das A., Prashar V., *et al.* Potential inhibitors against papain-like protease of novel coronavirus (SARS-CoV-2) from FDA approved drugs. *ChemRxiv*. Cambridge: Cambridge Open Engage; 2020.
- [14] Sharma J., Khurana N., Sharma N., *et al.* Phytochemical evaluation and antioxidant screening studies of ocimumtenuiflorumlinn seeds. *Asian journal of pharmaceutical and clinical*

- research, 2017; 76-82.
- [15] Narkhede RR., Cheke RS., Ambhore JP., *et al.* The molecular docking study of potential drug candidates showing Anti-COVID-19 activity by exploring therapeutic targets of SARS-CoV-2. *European Medical journal oncology*, 2020; 4(3):185-195.
<https://doi.org/10.14744/ejmo.2020.31503>.
- [16] Khaerunnisa S., Kurniawan H., Awaluddin R., *et al.* Potential inhibitor of COVID-19 main protease (M^{pro}) from several medicinal plant compounds by molecular docking. *Preprints* 2020, 2020030226.
<https://doi.org/10.20944/preprints202003.0226.v1>.
- [17] Hall Jr DC. and Ji HF. A search for medications to treat COVID-19 via *insilico* molecular docking models of the SARS-CoV-2 spike glycoprotein and 3CL Protease. *Travel Medicine and Infectious disease*, 2020;
<https://doi.org/10.1016/j.tmaid.2020.101646>.
- [18] Wang Q., Wu J., Wang H., *et al.* Structural basis for RNA replication by the SARS-CoV-2 Polymerase. *Cell*, 2020.
<https://doi.org/10.1016/j.cell.2020.05.034>.
- [19] Dipti M. and Ramesh KV. Binding site analysis of potential protease inhibitors of COVID-19 using autodock. *Virusdisease*, 2020;
<https://doi.org/10.1007/s13337-020-00585-z>.
- [20] Khataniar A., Pathak U., Rajkhowa S., *et al.* A Comprehensive Review of Drug Repurposing Strategies against Known Drug Targets of COVID-19. *COVID*. 2022; 2(2):148-167.
<https://doi.org/10.3390/covid2020011>.
- [21] Omkar I., Ajit Kumar S., Deeksha T., *et al.* Deciphering antiviral efficacy of malaria box compounds against malaria exacerbating viral pathogens- Epstein Barr virus and SARS-CoV-2, an in silico study. *Medicine in Drug Discovery*, 2022; 16:1-10.
- [22] Savita M. K., Bora N., Singh R., *et al.* Screening of camphene as a potential inhibitor targeting SARS – CoV2 various structural and functional mutants: Through reverse docking approach, *Environmental health Engineering and Management journal*, 2023; 10(2):123-129.
- [23] Jayaram, B., Singh, T., Mukherjee, G., *et al.* Sanjeevini: a freely accessible web-server for target directed lead molecule discovery. *BMC Bioinformatics* **13**(Suppl 17), S7(2012).
<https://doi.org/10.1186/1471-2105-13-S17-S7>.
- [24] Nelson C. A., Minasov G., Shuvalova L., *et al.* Structure of the SARS-CoV-2 ORF7A encoded accessory protein. *RCSB Protein Data Bank (PDB)*, 2020.
<https://doi.org/10.2210/pdb6W37/pdb>.
- [25] Michalska K., Kim Y., Jedrzejczak R., *et al.* A Crystal structures of SARS-CoV-2 ADP-ribose phosphatase: from the apo form to ligand complexes. *International Union crystallography journal*. 2020; 7(5):814-824.
<https://doi.org/10.1107/S2052252520009653>. PMID: 32939273; PMCID: PMC7467174.
- [26] Yan L. M., Huang Y. C., Lou Z. Y., *et al.* Crystal structure of 2019-nCov nsp16-nsp10 complex. *RCSB Protein Data Bank (PDB)*, 2020.
<https://doi.org/10.2210/pdb7BQ7/pdb>.
- [27] David M. Kern, Ben Sorum, Sonali S. Mali, *et al.* Cryo-EM structure of the SARS-CoV-2 3a ion channel in lipid nanodiscs. *Nature Structural & Molecular Biology*, 2020; 18:2020.06.17.156554.
<https://doi.org/10.1101/2020.06.17.156554>. PMID: 32587976; PMCID: PMC7310636.
- [28] Waugh W A. and King C G. Isolation and identification of Vitamin C. *Journal of biological chemistry*, 1932; 97:325-331.
- [29] Wong YC., Ahmad-Mudzaqqir M. Y., Wan-Nurdiyana W. A. Extraction of essential oil from Cinnamon (*Cinnamoumzeylanicum*). *Oriental journal of chemistry*, 2014; 30:37-47.
- [30] Ashok Pawar H., Jagannath A., Chooudry P. D. A novel and simple approach for extraction and isolation of curcuminoids from turmeric rhizomes. *Natural product research*, 2017; 6:1-4.
- [31] Johnson S., Morgan DE., Peiris CN. Development of the major triterpenoids and oil in the fruit and seeds of Neem (*Azadirachta indica*). *Annals of botany*, 1996; 78:383-386.
- [32] Rao PS, Midde NM, Miller DD, *et al.* Diallyl sulphide: Potential use in novel therapeutic interventions in alcohol, drugs, and disease mediated cellular toxicity by targeting cytochrome P450 2E1. *Current drug metabolism*, 2015; 16(6):486-503.
<https://doi.org/10.2174/138920021666615081213554>.

- [33] Widyat W., Hadiyanto H., Cahyono B., *et al.* Optimization of eugenol extraction of clove oil using response surface methodology. *Modern applied science*, 2015; 9:68-76.
- [34] Ghasemzadeh A., Jaafar H.Z. and Rahmat, A. Optimization protocol for the extraction of 6-gingerol and 6-shogaol from zingiber officinale var. rubrum theilade and improving antioxidant and anticancer activity using response surface methodology. *BMC complementary and alternative medicine*, 2015; 15:258.
<https://doi.org/10.1186/s12906-015-0718-0>.
- [35] Cid-Ortega S. and Monroy-rivera J. A. Extraction of kaempferol and its glycosides using supercritical fluids from plant sources: A review. *Food technology and biotechnology*, 2018; 56(4): 480-493.
<https://doi.org/10.17113/ftb.56.04.18.5870>.
- [36] Pholphana N., Rangkadilok N., Saehun J., *et al.* Changes in the contents of four active diterpenoids at different growth stages in *Andrographis paniculata* (Burm.f.) Nees (Chuan Xin Lian). *Chinese Medicine*, 2013; 8:1-12.
- [37] Gorgani L., Mohammadi M., Najafpor GD., *et al.* The piperine-The bioactive compound of black pepper: from isolation to medicinal formulations. *Comprehensive reviews in food safety and food reviews*, 2017; 16:124-140.
<https://doi.org/10.1111/1541-4337.12246>.
- [38] Domanska U., Wisniewska A. and Dabrowski A. Extraction of quercetin from red onion (*Allium cepa*L.) with ionic liquids, *Chromatography and separation technique journal*, 2018; 1:1-6.
- [39] Sharma J., Khurana N., Sharma N., *et al.* Phytochemical evaluation and antioxidant screening studies of *Ocimum tenuiflorum* Linn seeds. *Asian journal of pharmaceutical and clinical research*, 2017; 10(16):76-82.
- [40] Forouzanfar F., Bazza BS. and Hosseinzadeh H. Black cumin (*Nigella sativa*) and its constituent (thymoquinone): a review on antimicrobial effects. *Iranian journal of basic medical sciences*, 2014; 17(12):929-938.
- [41] Keesara BR. and Jar R. K. Isolation and characterization of vasicine from *Adathodavasica* (Adusa). *International journal of research and development in pharmacy and life sciences*, 2017; 6(2):2590-2596.